

# Controlled delivery of $\beta$ -globin-targeting TALENs and CRISPR/Cas9 into mammalian cells for genome editing using microinjection

Renee N. Cottle, Ciaran M. Lee, David Archer, and Gang Bao

## Supplementary Information Contents

**Supplementary Figure 1.** Microinjected K562 cells on retronectin coated polystyrene dishes.

**Supplementary Figure 2.** Gene expression efficiency in K562 cells.

**Supplementary Figure 3.** Separation of microinjected K562 cells using FACS.

**Supplementary Figure 4.** K562 cell doubling time after microinjection and nucleofection.

**Supplementary Figure 5.** T7E1 mutation detection assays for L4-R4 TALENs targeting *HBB* and off-target indels at *HBD*.

**Supplementary Figure 6.** Efficiency for sorting single cells by FACS.

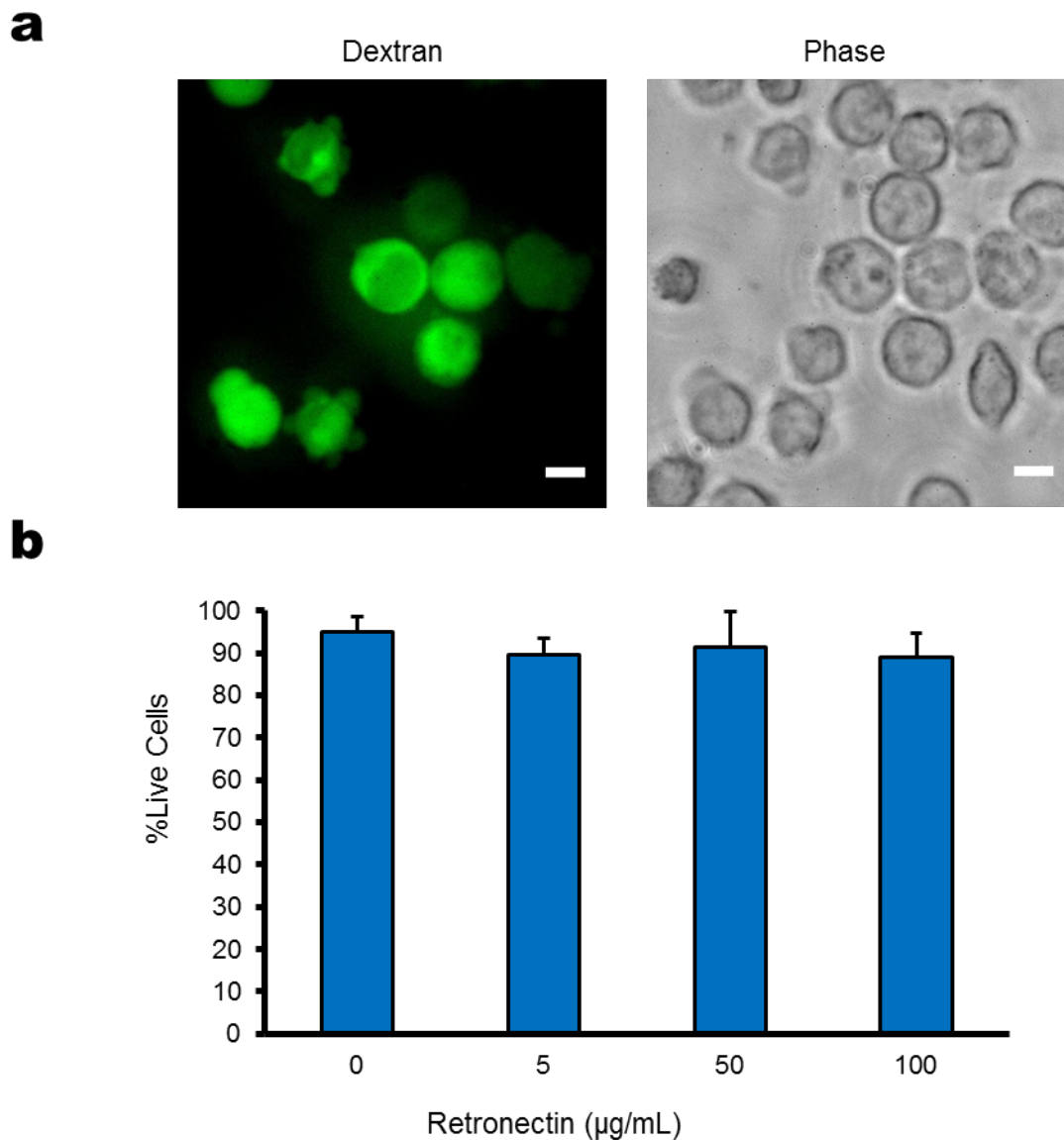
**Supplementary Figure 7.** Indel spectrum in K562 cells nucleofected with R02 CRISPR/Cas9.

**Supplementary Table 1.** Sequences of primers used to amplify the endogenous genes for T7E1 mutation detection assays.

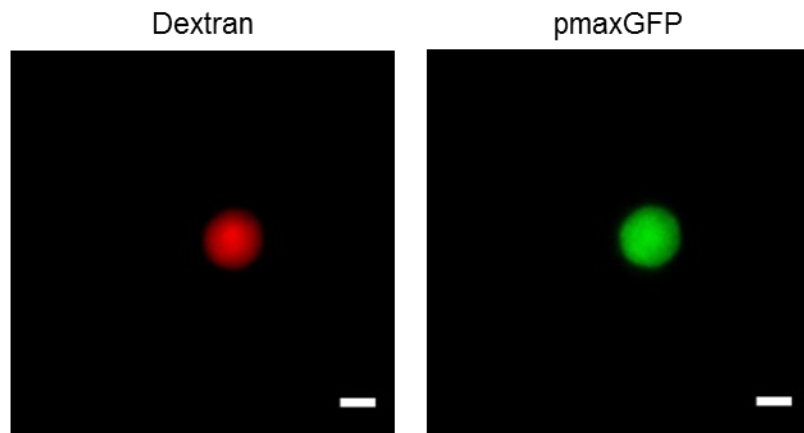
**Supplementary Table 2.** Sequences of primers used for PCR confirmation of HDR-mediated GFP integration in *HBB*.

**Supplementary Table 3.** Sequences of primers used for amplifying *HBB* in single cell clones for T7E1 assay and Sanger sequencing.

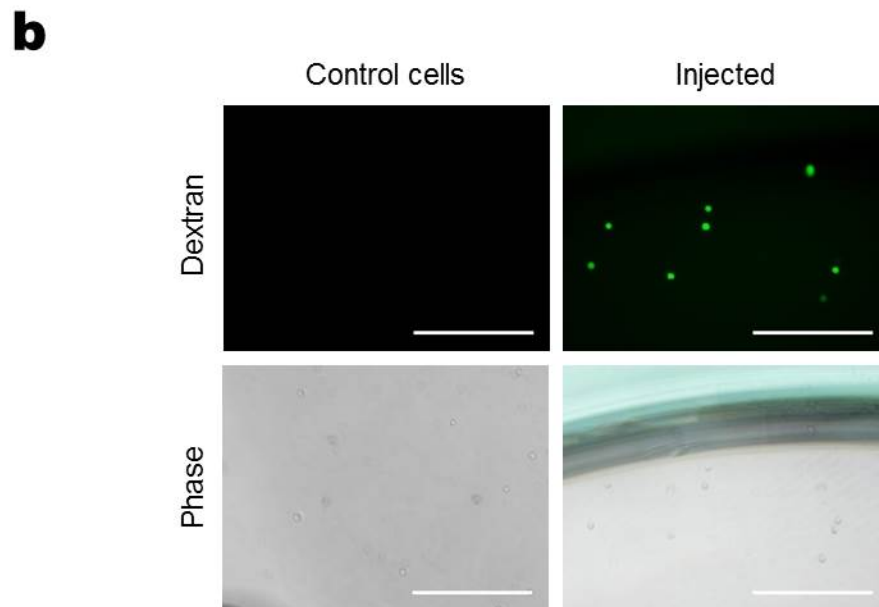
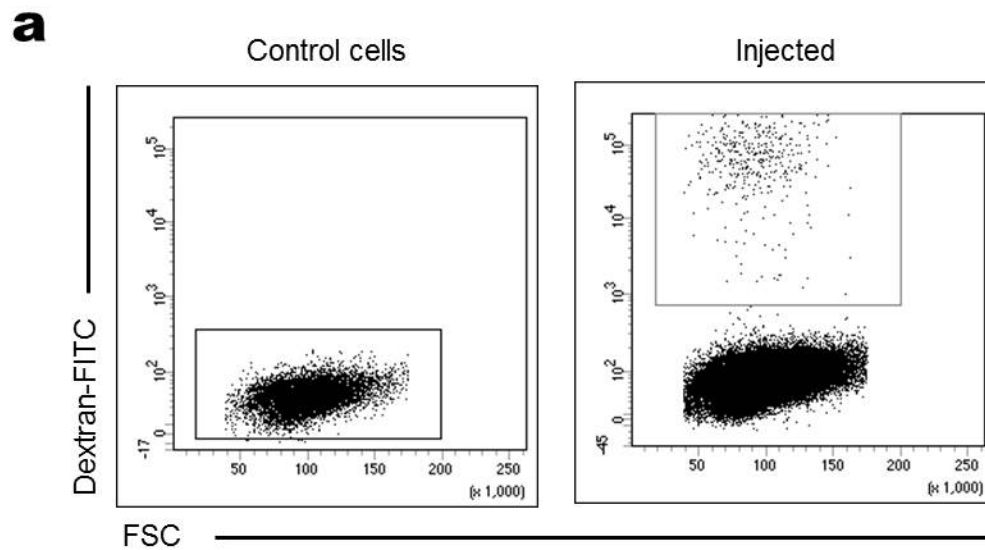
**Supplementary Table 4.** Analysis of clones with on- and off-target activity.



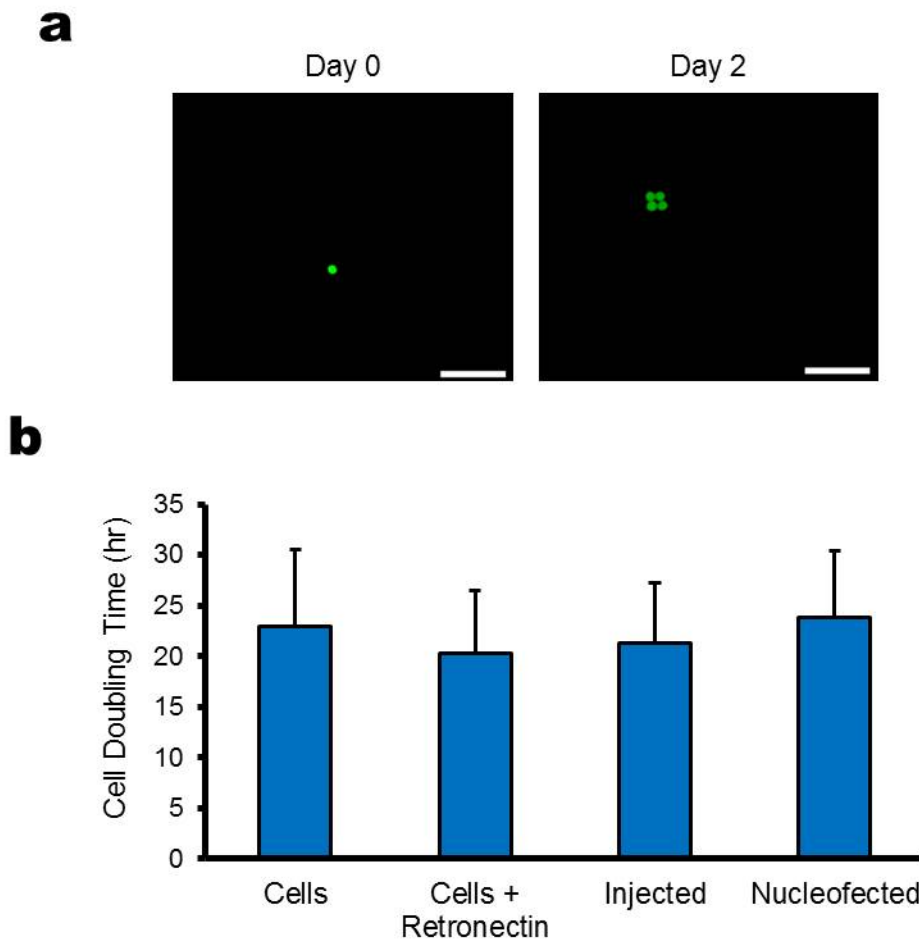
**Supplementary Figure 1.** Microinjected K562 cells on retronectin coated polystyrene dishes. **(a)** Fluorescence and phase contrast microscopy images of successfully injected cells immediately following injection with FITC-dextran. **(b)** Cell viability was not affected by retronectin as shown by the percentage of live cells detached from dishes coated with solutions containing different initial retronectin concentrations. For each sample,  $3 \times 10^4$  cells attached to coated dishes were detached using pipetting. Bars represent statistical mean for 3 replicates  $\pm$  the standard deviation. Scale bar width corresponds to 10  $\mu$ m.

**a****b**

**Supplementary Figure 2.** Gene expression efficiency in K562 cells **(a)** Fluorescence microscopy images of K562 cells injected with TRITC-dextran and pmaxGFP plasmid at 24 hours after injection. Cells with successful injections (red) were analyzed for GFP expression (green). **(b)** Phase contrast image of K562 cells on a retronectin coated surface. The white arrows indicate the debris from a cell damaged by injection. Scale bar width corresponds to 10  $\mu\text{m}$ .

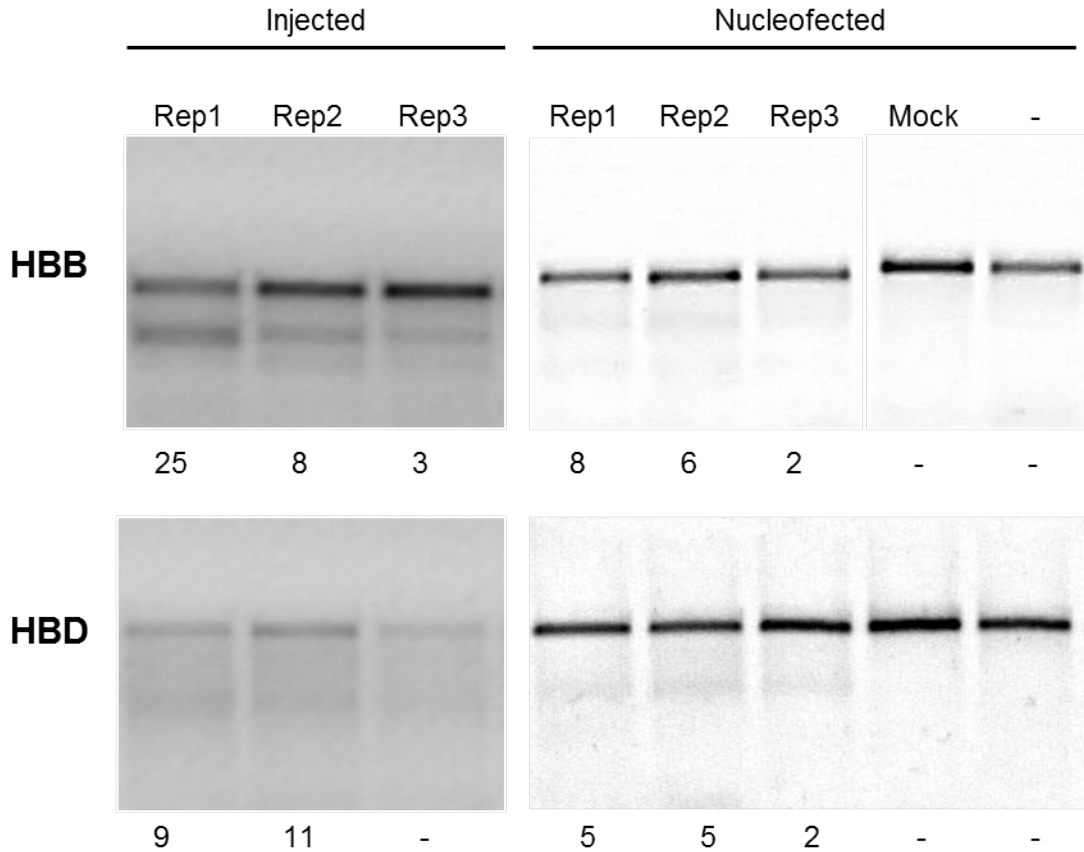


**Supplementary Figure 3.** Separation of microinjected K562 cells using FACS. Cells injected with FITC-dextran were detached from retronectin coated dishes after injection and subjected to FACS. **(a)** Panels show stable dextran fluorescence in cells gated for viability. For clarity, the control and injected K562 cells are shown in black and gray boxes respectively. **(b)** Fluorescence and phase microscopy images of injected and control cells after FACS. Scale bar width corresponds to 500  $\mu\text{m}$

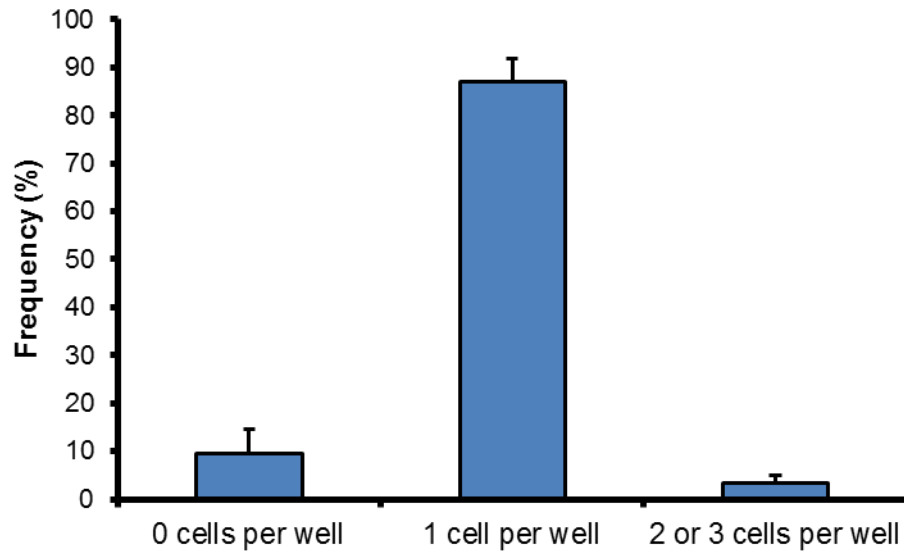


**Supplementary Figure 4.** K562 cell doubling time after microinjection and nucleofection. Viable K562 cells were deposited as single cells into Terasaki MicroWell plates using FACS at 24 hours after injection of FITC-dextran or nucleofection of pmaxGFP. **(a)** Fluorescence microscopy images of injected cells at 0 hours and 48 hours after FACS. **(b)** Plot of the cell doubling time for viable control and treated cells. The cell doubling time was calculated using the equation: incubation time between scoring cells  $\times \ln 2$  divided by  $\ln \frac{x_e}{x_b}$ , where  $x_e$  is the cell number at 48 hours and  $x_b$  is the cell number at 24 hours. As controls, we show the cell doubling time for viable untreated cells in suspension and detached from retronectin coated plates. One-way ANOVA indicates absence of a significant difference between different

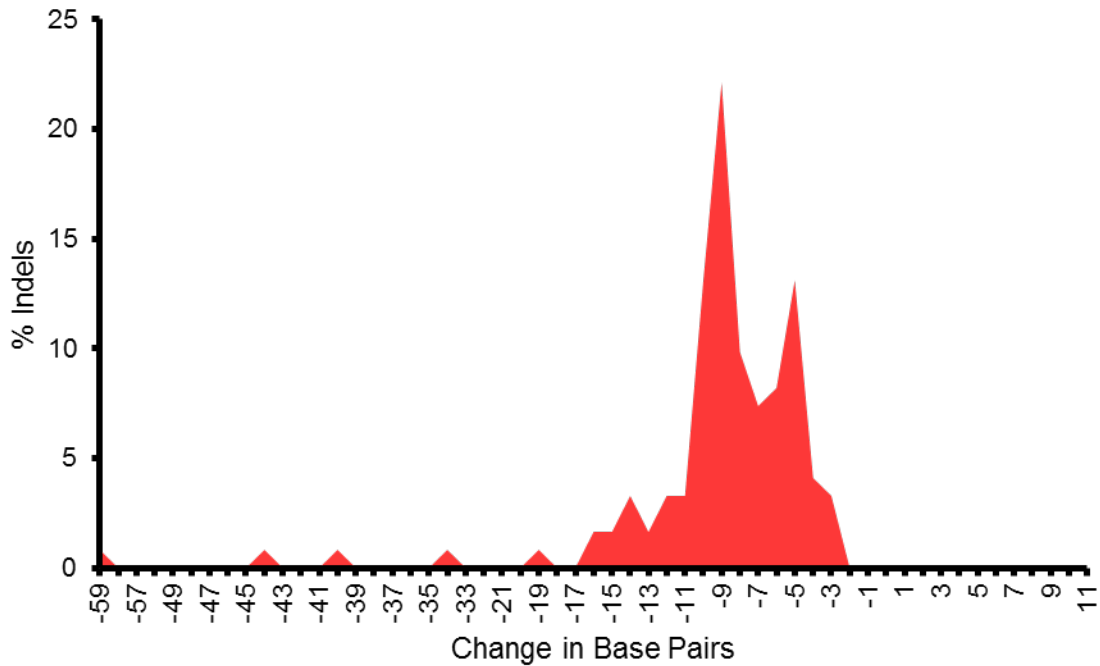
conditions ( $p > \alpha$ ,  $\alpha = 0.05$ ). Scale bar width corresponds to 100  $\mu\text{m}$ . Bars represent mean cell doubling time  $\pm$  standard deviation ( $n = 3$ ).



**Supplementary Figure 5** T7E1 mutation detection assays for L4-R4 TALENs targeting *HBB* and off-target indels at *HBD*. K562 cells were microinjected or nucleofected with L4-R4 expressing plasmids. Experiments were repeated 3 times. The detectable indel percentages are shown below each lane.



**Supplementary Figure 6.** Efficiency for sorting single cells by FACS. eGFP<sup>+</sup> Lin<sup>-</sup>Sca-1<sup>+</sup>kit<sup>+</sup> cells were single cell sorted into 66 wells of a Terasaki MicroWell dish. We counted the number of cells in each well using fluorescence microscopy. Up to 3 cells was counted for each well. The bars represent the mean percentage of wells that contained 0, 1, or 2 and more cells  $\pm$  the standard deviation, n = 4.



**Supplementary Figure 7.** Indel spectrum in K562 cells nucleofected with R02 CRISPR/Cas9. K562 cells ( $2 \times 10^5$ ) were nucleofected with 1  $\mu\text{g}$  of plasmid encoding for the R02 CRISPR/Cas9 nuclease and then analyzed using a custom SMRT sequencing analysis pipeline. The change in the number of base pairs resulting from NHEJ repair of DNA cleavage in *HBB* was compiled for each sequence read. The y-axis represents the percentage of indels with specified number of base pair changes.



Gene	Sequence
HBB-F	AGGCACCGAGCACTTTCTTGCC
HBB-R	ACCCTGTGGAGCCACACCCTA
HBD-F	GAGGTTGTCCAGGTGAGCCAGGCCATCAC
HBD-R	CTGCTGAAAGAGATGCGGTGGGGAGATATGTA
GRIN3A-F	GTTTCTAAGAGCGGTGGCTCTCA
GRIN3A-R	CTGCCCATCTATGCTTGGGA

**Supplementary Table 1.** Sequences of primers used to amplify the endogenous genes for the T7E1 mutation detection assays.

Gene	Sequence
GFP Integration-F	CGACAACCACTACCTGAGCA
GFP Integration-R	AGCAGAATGGTAGCTGGATTG
HBB Control-F	TGGTGGTGAGGCCCTGGGCAGGTTG
HBB Control-R	TAAAAGCAGAATGGTAGCTGGATT

**Supplementary Table 2.** Sequences of primers used for PCR confirmation of HDR-mediated GFP integration in *HBB*. The control primers for amplifying the *HBB* are also shown in the table.

Primer	Sequence
Beta 4F-Tag1	atcgAGGCACCGAGCACTTTCTTGCC
Beta 4F-Tag2	cagaAGGCACCGAGCACTTTCTTGCC
Beta 4F-Tag3	gctaAGGCACCGAGCACTTTCTTGCC
Beta 4F-Tag4	tgacAGGCACCGAGCACTTTCTTGCC
Beta 4F-Tag5	acgtAGGCACCGAGCACTTTCTTGCC
Beta 4F-Tag6	catgAGGCACCGAGCACTTTCTTGCC
Beta 4F-Tag7	gtgaAGGCACCGAGCACTTTCTTGCC
Beta 4F-Tag8	tagcAGGCACCGAGCACTTTCTTGCC
Beta 4F-Tag9	agtcAGGCACCGAGCACTTTCTTGCC
Beta 4R-Tag1	atcgACCCTGTGGAGCCACACCCTA
Beta 4R-Tag2	cagaACCCTGTGGAGCCACACCCTA
Beta 4R-Tag3	gctaACCCTGTGGAGCCACACCCTA
Beta 4R-Tag4	tgacACCCTGTGGAGCCACACCCTA
Beta 4R-Tag5	acgtACCCTGTGGAGCCACACCCTA
Beta 4R-Tag6	catgACCCTGTGGAGCCACACCCTA
Beta 4R-Tag7	gtgaACCCTGTGGAGCCACACCCTA
Beta 4R-Tag8	tagcACCCTGTGGAGCCACACCCTA
Beta 4R-Tag9	agtcACCCTGTGGAGCCACACCCTA

**Supplementary Table 3.** Sequences of primers used for amplifying *HBB* in single cell clones for the T7E1 assay and Sanger sequencing. Unique barcodes used to identify each clone is shown in lowercase.

	R02	L4-R4
Total Clones analyzed by T7E1	78	53
% Clones with on- and off-target activity	32.1	13.2
% Clones with on-target activity only	14.1	15.1
% Clones with off-target activity only	6.4	11.3

**Supplementary Table 4.** Analysis of clones with on- and off-target activity. Clones derived from single cells injected with R02 CRISPR/Cas9 or L4-R4 TALENs were analyzed for on- and off-

target activity using the T7E1 indel detection assay. The percentage of clones having on-target indels with and without off-target indels, or off-target indels only is shown in the table for each nuclease.